Stress Analysis in AAA does not Predict Rupture Location Correctly in Patients with Intraluminal Thrombus

Fanny Lorandon, Simon Rinckenbach, Nicla Settembre, Eric Steinmetz, Lucie Salomon Du Mont, Stéphane Avril

Title page

Stress analysis in AAA does not predict rupture location correctly in patients with intraluminal thrombus

Title page

Fanny Lorandon, MD[a*], Simon Rinckenbach, MD,PhD [a,b], Nicla Settembre, MD, PhD[c], Eric Steinmetz, MD,PhD[d], Lucie Salomon Du Mont, MD,PhD [a,b], Stephane Avril, PhD[e], Saint Etienne, France[e]

[a] Department of Vascular and Endovascular Surgery, University Hospital of Besançon, 25030 Besançon, France

[b] EA3920, University Hospital of Besançon, 25030 Besançon, France

[c] Department of Vascular Surgery, University Hospital of Nancy, Nancy, France

[d] Department of Vascular Surgery, University Hospital of Dijon, 21000 Dijon, France

[e]Mines Saint-Etienne, Univ Lyon, INSERM, U 1059 Sainbiose, Centre CIS, F - 42023 Saint-Etienne France (e-mail: avril@emse.fr)

Corresponding author:

Doctor Fanny Lorandon

Departement of vascular surgery

Centre Hospitalier Regional de Besancon

22 Boulevard Alexandre Fleming

23 25000 Besancon

24 florandon@chu-besancon.fr

25

Abstract and key words

Objectives

A biomechanical approach to the rupture risk of an abdominal aortic aneurysm (AAA) could be a solution to ensure a personalized estimate of this risk. It is still difficult to know in what conditions, the assumptions made by biomechanics, are valid. The objective of this work was to determine the individual biomechanical rupture threshold and to assess the correlation between their rupture sites and the locations of their maximum stress comparing two computed tomography scan (CT) before and at time of rupture.

Materials and Methods

We included 5 patients who had undergone two CT; one within the last 6 months period before rupture and a second CT scan just before the surgical procedure for the rupture. All DICOM data, both pre- and rupture, were processed following the same following steps: generation of a 3D geometry of the AAA, meshing and computational stress analysis using the finite element method. We used two different modelling scenarios to study the distribution of the stresses, a “wall” model without intraluminal thrombus (ILT) and a “thrombus” model with ILT.

Results

The average time between the pre-rupture and rupture CT scans was 44 days (22-97). The median of the maximum stresses applied to the wall between the pre-rupture and rupture states were 0.817 MPa (0.555-1.295) and 1.160 MPa (0.633-1.625) for the "wall" model; and 0.365 MPa (0.291-0.753) and 0.390 MPa (0.343-0.819) for the "thrombus" model. There was an

agreement between the site of rupture and the location of maximum stress for only one patient, who was the only patient without ILT.

Conclusion

We observed a large variability of stress values at rupture sites between patients. The rupture threshold strongly varied between individuals depending on the intraluminal thrombus. The site of rupture did not correlate with the maximum stress except for one patient.

Key words: Peak wall stress, Finite Element Analyses, Ruptured abdominal aortic aneurysm

Introduction

The challenge in managing patients with aortic aneurysms is to estimate the relationship between the surgical risk and the benefit of no rupture. Actually, defining the rupture risk of an asymptomatic or symptomatic abdominal aortic aneurysm (AAA) is essential for patients with this condition. By consensus, a maximum aneurysm diameter of 55 mm represents the current surgical indication for AAA.[1-3] However, this diameter threshold does not consider inter-individual variability. Indeed, small aneurysms may also be prone to rupture, while very large aneurysms may be observed without any symptoms.[1,4]

Numerical simulation using Finite Element Analyses (FEA) is an approach that could enable the prediction of rupture risks. Rupture of an aneurysm occurs when the local wall stress exceeds the local wall strength. Mechanical stresses mostly depend on the luminal pressure and on the arterial geometry, whereas the wall strength is a patient-specific material property. The latter being unknown, research focused on stress estimation. Several studies highlighted the relevance of biomechanical markers to estimate a risk of rupture by integrating factors such as patient geometry and characteristics into biomechanical criteria.[5-10] However, although they are statistically relevant, the significance of biomechanical markers at the individual level remains to be demonstrated.

Moreover, the mechanisms leading to ruptures are not yet completely understood. Identifying the mechanism of rupture would enable to define more precisely an individual risk of rupture. A biomechanical approach to the rupture risk of an abdominal aortic aneurysm (AAA) could be a solution to ensure a personalized estimate of this risk. It is still difficult to know in what conditions, the assumptions made by biomechanics, are valid.

The objective of this work was to determine the individual biomechanical rupture threshold and to assess the correlation between their rupture sites and the locations of their maximum stress comparing two Computed tomography (CT) scan before and at time of rupture.

Materials and Methods

We have conducted a retrospective study. The FEA method was applied to perform stress analyses on 5 patients who had a CT scan at the time of rupture and a CT scan within the 6 months prior to rupture. The use of these scan datasets permitted studying the evolution of the stresses of an AAA in the 6 months preceding the rupture.

Study population

Between 2010 and 2017, all patients who were managed urgently in the Vascular Surgery Department of Nancy, Dijon or Besancon for ruptured AAA were studied. Only patients treated for ruptured abdominal aortic aneurysm with CT scan diagnosis were taken into account. They also had to have an abdominal CT scan done in the 6 months before rupture to be included. CT scans of ruptured AAA revealed an extravasation of contrast material associated with an intra- or retroperitoneal hematoma. Any patient with a posterior aneurysmal rupture or associated with infectious or inflammatory aorta was excluded. We decided to study only patients with a case of anterior or lateral rupture. Chronic posterior ruptures are partly related to friction with vertebral bodies and are therefore part of a different biomechanical failure mechanism.[11] We chose to exclude posterior aneurysm rupture as, according to current theory, the spine plays a critical role in the posterial rupture[12,13] but it was not incorporated in our model. The failure sites were then identified, when it was possible to visualize a contrast extravasation.[14]

Computational modelling

The same protocol was applied for all models: generation of a 3D geometry of the lumen and thrombus of the AAA, volume meshing, and calculation of biomechanical criteria. (Figure 1) We chose to study a model without thrombus and a model with thrombus. The aneurysmal wall was modelled with shell elements[15] whereas the thrombus was modelled with solid elements. FEA were performed by a single investigator.

Segmentation

Simpleware™ ScanIP (Version N-2018.03-SP1; Synopsys, Inc., Mountain View, USA) was used to process CT DICOM datasets. The data were segmented in a semi-automatic way, based on thresholding criteria. For each CT scan, we segmented the lumen and thrombus of the AAA between the renal arteries and the aortic bifurcation. The segmentation of ruptured AAAs excluded the extra peritoneal hematoma which was identified thanks to the lower concentration of contrast agent after the haemorrhagic shock. The smoothing factor for all cases was assumed to be the same.

Mesh

The Synopsys' Simpleware™ FE module was used for volumetric mesh generation. Each 3D geometry was meshed using quadratic tetrahedral 3D elements. A previous mesh size study permitted to determine the optimal mesh size, with about 150 000 nodes and 160 000 elements for each FEA.

Finite Element Analysis

FEA were conducted using the Abaqus/CAE 2018 software (Dassault Systemes, SIMULIA, RI, USA).

We used two different modelling scenarios to study stress distributions. In the first scenario, the model consisted of a wall part, the pressure being applied onto it. In the second scenario, the model consisted of a wall part and a thrombus part. The pressure was applied on the inner surface.

To create the wall part from Abaqus, a membrane composed of STRI65 elements was applied to the entire aneurysm to reproduce the aortic wall, defined with a thickness of 1.5 mm.[8]

The thrombus part consisted of C3D10 elements. It was assumed to be completely tied to the wall part by merging the common nodes of the boundary.

Such analysis on AAA usually requires computing the zero-pressure geometry of the aorta. Since such computation can only be achieved when the patient-specific material properties are known, we preferred using the assumption proposed by Joldes et al. They performed the stress analysis using linear elastic behaviour and infinitesimal strains, ratio between wall stiffness and thrombus stiffness should be about 20:1. The wall part was assigned a Young's modulus of 100 000 MPa, and a Poisson's ratio of 0.48. The thrombus part was assigned a Young's modulus of 50 000 MPa and a Poisson's ratio of 0.48.[16,17] We used a 2:1 ratio and verified that the 2:1 ratio and the 20:1 ratios gave the same location of the peak wall stress.

The same boundary conditions were assigned to the 10 cases (5 patients, pre- and rupture analyses). A uniform blood pressure was applied onto the luminal surface (120mmHg). The AAA was fixed at the renal arteries and the aortic bifurcation. It was assumed that there was no contact with neighbouring organs.

After performing the stress analysis, the following criteria were recorded: the mean of Peak Wall Stress (PWS), the 99th percentile of the PWS. The considered stress component was the

first principal component. We used pre-rupture CT geometries to derive the peak wall stress and only used the post-rupture CT scan to compare rupture locations and peak stress locations.

Statistical Analysis

We conducted an observational analysis. Quantitative data were expressed as median (minimum-maximum) and qualitative data were expressed as numbers (percentage).

Results

We retrospectively identified 5 patients corresponding to our inclusion criteria (Figure 2). One patient came from the University hospital of Nancy, one patient came from the University hospital of Besancon and three patients came from the University hospital of Dijon. We included 5 patients, all men, who had a median age of 72 years (61-79). There was no history of diabetes, renal impairment or stroke. Four patients presented hypertension, five were smokers, two with dyslipidemia, coronary artery disease and peripheral arterial occlusive disease.

FEA were performed on 5 asymptomatic AAA, which ruptured secondarily. The median time between the pre-rupture and rupture CT scans was 44 days (22-97). The AAA of Patient 1 had the characteristic of not presenting an intra-luminal thrombus (ILT).

Table I shows FEA calculated parameters. Pre-rupture and rupture FEAs were compared with the “thrombus” model and with the “wall” model. Respectively, the median was 0.365 MPa (0.291-0.753) and 0.390 MPa (0.343-0.819) for the “thrombus” model. The median was 0.817 MPa (0.555-1.295) and 1.160 MPa (0.633-1.625) for the “wall” model. The stresses observed on the “thrombus model” were higher in rupture than in pre-rupture stage, from 2.4 % to 96.7

%, without any link to the delay between the two CT scans. This was also observed in the "wall" model, from 8.8 % to 98.9 %, with the exception of one patient. In this "wall" model, the stresses were reduced by 10% for patient 4 in comparison with rupture. The stresses were marginally higher in the wall model compared to the thrombus model, from 83-254% range for the pre-rupture stage to 85-270% for the rupture stage. The rupture occurred for different inhomogeneous stress values. It was not possible to define a common stress threshold value for each AAA. Concerning the stress distribution, it seemed more obvious to find agreements in the wall model compared to the thrombus model (Figure 3 and 4).

The site of rupture was not visible for patient 4. For other patients, the rupture site was visualized by contrast extravasation, wall continuity solution or intra-thrombus haemorrhage. There was an agreement between PWS and rupture site for a single patient (patient 1), the one who had the particularity of not presenting ILT. (Table I) (Figure 5)

Discussion

Rupture threshold

FEA can predict the rupture risk of an AAA for a predefined blood pressure.[18] Through this work, we wanted to study more precisely the evolution of the peak wall stress based on pre-ruptured and ruptured scanographic data of AAA within a short period of 6 months preceding the rupture. There are only 2 other studies comparing pre-rupture and rupture CT scans of the same patients, but the time between aneurysm rupture and the pre-rupture scan was significantly larger: 308 days for the work of *Erhart et al*[14] and 731 days for the work of *Jalalzadeh et al*[19].

As expected, the stresses values of the rupture stage were larger than the pre-rupture stage. These results were consistent with the work of *Erhart et al*.[20]

192 The results of the study show a great dispersion of the stress values at rupture as well as a
193 variability of the evolution during the last six months preceding the rupture. The rupture
194 occurred for different stress values, with variations ranging from single to double. The rupture
195 stress value seems intrinsically patient specific. This could easily be explained by the fact that
196 strength values may vary significantly with the thrombus geometry, which was shown to play
197 a prominent role on the proteolytic activity of the wall.[6,21,22] The study of the stress distribution
198 of an AAA represents an indirect sign of rupture risk. This study does not allow to estimate the
199 individual risk of rupture. The wall strength has to be determined in order to derive an individual
200 risk. It should be highlighted that the largest stresses were predicted in the absence of thrombus.
201 This could indicate a shielding role of the thrombus.[23] This would also confirm the role of the
202 thrombus in causing indirectly a decrease of the wall strength due to the increased proteolytic
203 activity. Accordingly, the wall model, though imperfect, can provide fast predictions. Published
204 models over the last 10 years have attempted to approach reality, but there is still a pressing
205 need of simple models that can estimate accurately AAA rupture risk.[24,25]

206 From the clinical point, these results have finally highlighted the need for ruptured or
207 symptomatic AAA hospitalized patients to maintain minimal systolic blood pressure under 70
208 -90 mmHg in order to decrease the stresses applied to the arterial wall.[26,27] Controlling the blood
209 pressure would give important indications about the risk of rupture.

210

211 **Correlation between rupture site and maximum stress**

212 We were able to find an agreement between the maximum stress location and the rupture site
213 for only one out of the five patients, the one without thrombus. For the other patients, none of
214 the models with or without ILT showed any correlation between the distribution of the
215 maximum stress and the rupture site. Some studies on small cohorts have studied the correlation

between PWS and rupture site. The results were contradictory. Some studies found a correlation between the rupture site and PWS or PWRR (PWS/Wall strength) location. [8,14,28] The fact that the PWS location and the rupture site agreed only for the thrombus-free patient could indicate that the thrombus would participate in a redistribution of the stresses applied to the wall, or that the thrombus would induce a local decrease of the wall strength due to larger proteolytic activity. Thus, the ILT could cause a change in the stresses applied to the aneurysmal wall and simultaneously a change of strength, related to its thickness and distribution. *Doyle et al* studied CT data of a secondarily ruptured case. They observed that, on the pre-rupture data, the peak wall stress was located on the rupture site. However, only one case was presented in their study, which was an AAA without thrombus.[29]

Metaxa et al[30] studied the failure site of an AAA. They were able to point out that the maximum stresses were located at the shoulders of the AAA and that the rupture occurred preferentially in the zone where the growth of the aneurysm was the most important. They also determined that the wall failure site did not coincide with the thrombus failure site. Thus, we could suggest that the maximum stresses were not a sufficient indicator for estimating the individual rupture risk. It appears that the patient-specific strength of the aneurysmal wall is needed to evaluate the rupture site, even when we have recent pre-rupture scans. Moreover, the thrombus plays an essential role on the stress distribution in the wall. The work of *Wang et al*[31] also showed that the thrombus thickness would influence the localization of the maximum stress and the stress distribution. In addition, the rupture location in the thrombus does not correspond exactly to the rupture location in the wall as demonstrated by *Metaxa et al*, which emphasizes the complexity of the role played by ILT.[30]

It was observed that rupture occurs preferentially in the posterolateral region, which is in agreement with our results (3 patients out of 4). This observation could be related to the external constraints applied onto the AAA.[4] Moreover, the effects of surrounding tissues, not accounted

for in our model, could explain the deviation between the actual rupture location and the location of peak wall stress. *Farsad et al*[13] investigated the role of the spine in the development of AAA, showing that it could promote anterior and posterolateral AAA progression. Therefore, the spine therefore has an impact on the distribution of stresses on the wall. This is in agreement with the work of *Kim et al*[32] on thoracic aortic aneurysms. They showed that the tissues surrounding the thoracic aorta should be taken into account when studying the stresses applied to the wall. Finally, studies on cerebral aneurysms have also highlighted the importance of the perianeurysmal tissue on rupture.[33]

As we applied a similar wall strength for all situations, we chose not to calculate the RPI.[34] Indeed, the RPI map would be similar to the stress map and the location of the peak wall stress would be the same as the location of peak RPI. A possible interesting future work would be to have regionally varying strength values to derive the RPI. However, assessing patient-specific and region-specific strength remains challenging.[35] These variabilities are the main reason explaining the discrepancy between the location of peak wall stress and the location of observed rupture.

Limitations of the model

The small sample size is a limitation of this work. We favored short times between the 2 scans over the sample size, unlike other studies where the time between aneurysm rupture and the pre-rupture scans was significantly larger.[14,19]

Material properties cannot be derived from CT scans so the same model was used for all patients. The model did not take into account wall calcifications, surrounding organs, wall thickness and layer-specific material properties. To overcome these limitations, we used the

Joldes approach[16], which did not require information on material properties and neglects geometric nonlinearities.[10,17,36,37]

ILT modeling does not take into account all the complexity of its composition and its role in AAA rupture. The complexity of ILT mechanics deserves future studies to evaluate how it affects the location of the peak wall stress in the wall.[38]

We decided to use the 99th percentile stress which was more reliable as a biomechanical imaging marker than PWS, in order to avoid all false positives related to segmentation defects.[39,40]

We assumed a uniform 1.5mm wall thickness as it was not possible to measure the thickness from CT scan data. However, adopting a constant wall thickness is one of the limitations of this work. Several studies [41-44] took into account the thickness of the wall to compute the wall stress in AAA. They observed that this had an impact on the distribution of stresses. Taking into account wall thickness could help to refine rupture site.

The remodeling related to the retro or intra-peritoneal hematoma complicated semi-automatic segmentation.

Due to lack of information, we had to apply a uniform blood pressure of 120 mmHg on all models. However, the occurrence of an AAA rupture leads to a state of hemorrhagic shock and therefore a modification of the stresses applied to the aneurysm wall.

Predictive biomechanical markers of rupture

While many studies have highlighted the superiority of biomechanical markers[10], the exact mechanism of AAA rupture is not yet known. It would seem that estimating such markers could be considered as indirect signs of increased risk of rupture. They could not be interpreted on an individual scale of risk of rupture.

To know to what stress the aneurysmal wall ruptures, it might be interesting to take into account the stress values for a non-aneurysmal wall portion of the same patient or to try to determine the site of the wall with the lowest strength.

Conclusion

In conclusion, rupture risk estimation for AAA based on PWS presented a large inter-individual variability and did not correlate with the rupture site. We submitted that the site of rupture was determined by the regional variations of the wall resistance rather than the wall maximum stress and that the ILT played a major role in these variations.

298 Acknowledgements

299 SA is grateful to the ERC through ERC-2014-CoG BIOLOCHANICS grant.

300

301 We did not ask for ethics committees as we were outside the Jardé law. There was no change

302 in current clinical practice.

303

304 References

305 1 Brewster DC, Cronenwett JL, Hallett JW, et al. Guidelines for the treatment of
306 abdominal aortic aneurysms. Report of a subcommittee of the Joint Council of the American
307 Association for Vascular Surgery and Society for Vascular Surgery. *J Vasc Surg*
308 2003;**37**(5):1106–17.

309 2 Moll FL, Powell JT, Fraedrich G, et al. Management of Abdominal Aortic Aneurysms
310 Clinical Practice Guidelines of the European Society for Vascular Surgery. *Eur J Vasc*
311 *Endovasc Surg* 2011;**41**:S1–58.

312 3 Chaikof EL, Dalman RL, Eskandari MK, et al. The Society for Vascular Surgery
313 practice guidelines on the care of patients with an abdominal aortic aneurysm. *J Vasc Surg*
314 2018;**67**(1):2-77.e2.

315 4 Darling RC, Messina CR, Brewster DC, et al. Autopsy study of unoperated abdominal
316 aortic aneurysms. The case for early resection. *Circulation* 1977;**56**(3 Suppl):II161-164.

317 5 Maier A, Gee MW, Reeps C, et al. A comparison of diameter, wall stress, and rupture
318 potential index for abdominal aortic aneurysm rupture risk prediction. *Ann Biomed Eng*
319 2010;**38**(10):3124–34.

320 6 Gasser TC. Biomechanical Rupture Risk Assessment: A Consistent and Objective
321 Decision-Making Tool for Abdominal Aortic Aneurysm Patients. *Aorta Stamford Conn*
322 2016;**4**(2):42–60.

323 7 Vande Geest JP, Di Martino ES, Bohra A, et al. A biomechanics-based rupture
324 potential index for abdominal aortic aneurysm risk assessment: demonstrative application.
325 *Ann N Y Acad Sci* 2006;**1085**:11–21.

326 8 Doyle BJ, Coyle P, Kavanagh EG, et al. A Finite Element Analysis Rupture Index
327 (FEARI) Assessment of Electively Repaired and Symptomatic/Ruptured Abdominal Aortic

Aneurysms. 6th World Congress of Biomechanics (WCB 2010). August 1-6, 2010 Singapore. Springer, Berlin, Heidelberg; 2010. pp. 883–6.

9 Leemans EL, Willems TP, van der Laan MJ, et al. Biomechanical Indices for Rupture Risk Estimation in Abdominal Aortic Aneurysms. *J Endovasc Ther* 2017;**24**(2):254–61.

10 Farotto D, Segers P, Meuris B, et al. The role of biomechanics in aortic aneurysm management: requirements, open problems and future prospects. *J Mech Behav Biomed Mater* 2018;**77**:295–307.

11 Wadgaonkar AD, Black JH, Weihe EK, et al. Abdominal aortic aneurysms revisited: MDCT with multiplanar reconstructions for identifying indicators of instability in the pre- and postoperative patient. *Radiographics* 2015;**35**(1):254–68.

12 Walker ST, Pipinos II, Johanning JM, et al. Contained Rupture of an Abdominal Aortic Aneurysm With Extensive Vertebral Body and Retroperitoneal Space Destruction. *J Comput Assist Tomogr* 2017;**41**(5):839–42.

13 Farsad M, Zeinali-Davarani S, Choi J, et al. Computational Growth and Remodeling of Abdominal Aortic Aneurysms Constrained by the Spine. *J Biomech Eng* 2015;**137**(9).

14 Erhart P, Roy J, de Vries J-PPM, et al. Prediction of Rupture Sites in Abdominal Aortic Aneurysms After Finite Element Analysis. *J Endovasc Ther* 2016;**23**(1):115–20.

15 Raut SS, Chandra S, Shum J, et al. The Role of Geometric and Biomechanical Factors in Abdominal Aortic Aneurysm Rupture Risk Assessment. *Ann Biomed Eng* 2013;**41**(7):1459–77.

16 Joldes GR, Miller K, Wittek A, et al. A simple, effective and clinically applicable method to compute abdominal aortic aneurysm wall stress. *J Mech Behav Biomed Mater* 2016;**58**:139–48.

17 Joldes GR, Miller K, Wittek A, et al. BioPARR: A software system for estimating the rupture potential index for abdominal aortic aneurysms. *Sci Rep* 2017;**7**(1):4641.

18 Fillinger MF, Marra SP, Raghavan ML, et al. Prediction of rupture risk in abdominal aortic aneurysm during observation: wall stress versus diameter. *J Vasc Surg* 2003;**37**(4):724–32.

19 Jalalzadeh H, Leemans EL, Indrakusuma R, et al. Estimation of Abdominal Aortic Aneurysm Rupture Risk with Biomechanical Imaging Markers. *J Vasc Interv Radiol* 2019;**30**(7):987-994.e4.

20 Erhart P, Hyhlik-Dürr A, Geisbüsch P, et al. Finite element analysis in asymptomatic, symptomatic, and ruptured abdominal aortic aneurysms: in search of new rupture risk predictors. *Eur J Vasc Endovasc Surg* 2015;**49**(3):239–45.

21 Stevens RRF, Grytsan A, Biasetti J, et al. Biomechanical changes during abdominal aortic aneurysm growth. *PloS One* 2017;**12**(11):e0187421.

22 Chauhan SS, Gutierrez CA, Thirugnanasambandam M, et al. The Association Between Geometry and Wall Stress in Emergently Repaired Abdominal Aortic Aneurysms. *Ann Biomed Eng* 2017;**45**(8):1908–16.

23 Kontopodis N, Koncar I, Tzirakis K, et al. Intraluminal thrombus deposition is reduced in ruptured compared to diameter matched intact abdominal aortic aneurysms. *Ann Vasc Surg* 2018.

24 Malkawi AH, Hinchliffe RJ, Xu Y, et al. Patient-specific biomechanical profiling in abdominal aortic aneurysm development and rupture. *J Vasc Surg* 2010;**52**(2):480–8.

25 Gasser TC, Auer M, Labruto F, et al. Biomechanical rupture risk assessment of abdominal aortic aneurysms: model complexity versus predictability of finite element

374 simulations. *Eur J Vasc Endovasc Surg* 2010;**40**(2):176–85.

375 26 Reimerink JJ, van der Laan MJ, Koelemay MJ, et al. Systematic review and meta-
376 analysis of population-based mortality from ruptured abdominal aortic aneurysm. *Br J Surg*
377 2013;**100**(11):1405–13.

378 27 Ohki T, Veith FJ. Endovascular Grafts and Other Image-Guided Catheter-Based
379 Adjuncts to Improve the Treatment of Ruptured Aortoiliac Aneurysms: *Ann Surg*
380 2000;**232**(4):466–79.

381 28 Venkatasubramaniam AK, Fagan MJ, Mehta T, et al. A comparative study of aortic
382 wall stress using finite element analysis for ruptured and non-ruptured abdominal aortic
383 aneurysms. *Eur J Vasc Endovasc Surg* 2004;**28**(2):168–76.

384 29 Doyle BJ, McGloughlin TM, Miller K, et al. Regions of high wall stress can predict
385 the future location of rupture of abdominal aortic aneurysm. *Cardiovasc Intervent Radiol*
386 2014;**37**(3):815–8.

387 30 Metaxa E, Tzirakis K, Kontopodis N, et al. Correlation of Intraluminal Thrombus
388 Deposition, Biomechanics, and Hemodynamics with Surface Growth and Rupture in
389 Abdominal Aortic Aneurysm-Application in a Clinical Paradigm. *Ann Vasc Surg*
390 2018;**46**:357–66.

391 31 Wang DHJ, Makaroun MS, Webster MW, et al. Effect of intraluminal thrombus on
392 wall stress in patient-specific models of abdominal aortic aneurysm. *J Vasc Surg*
393 2002;**36**(3):598–604.

394 32 Kim J, Peruski B, Hunley C, et al. Influence of surrounding tissues on biomechanics of
395 aortic wall. *Int J Exp Comput Biomech* 2013;**2**(2):105–17.

396 33 Sugiu K, Jean B, San Millan Ruiz D, et al. Influence of the perianeurysmal

environment on rupture of cerebral aneurysms. Preliminary observation. *Interv Neuroradiol J*2000;**6 Suppl 1**:65–70.

34 Vande Geest JP, Di Martino ES, Bohra A, et al. A biomechanics-based rupture potential index for abdominal aortic aneurysm risk assessment: demonstrative application. *Ann N Y Acad Sci* 2006;**1085**:11–21.

35 Azar D, Ohadi D, Rachev A, et al. Mechanical and geometrical determinants of wall stress in abdominal aortic aneurysms: A computational study. *PloS One* 2018;**13**(2):e0192032.

36 Novak K, Polzer S, Bursa J. Applicability of simplified computational models in prediction of peak wall stress in abdominal aortic aneurysms. *Technol Health Care* 2017.

37 Kontopodis N, Metaxa E, Papaharilaou Y, et al. Advancements in identifying biomechanical determinants for abdominal aortic aneurysm rupture. *Vascular* 2015;**23**(1):65–77.

38 O'Leary SA, Kavanagh EG, Grace PA, et al. The biaxial mechanical behaviour of abdominal aortic aneurysm intraluminal thrombus: classification of morphology and the determination of layer and region specific properties. *J Biomech* 2014;**47**(6):1430–7.

39 Indrakusuma R, Jalalzadeh H, Planken RN, et al. Biomechanical Imaging Markers as Predictors of Abdominal Aortic Aneurysm Growth or Rupture: A Systematic Review. *Eur J Vasc Endovasc Surg* 2016;**52**(4):475–86.

40 Speelman L, Bosboom EMH, Schurink GWH, et al. Patient-specific AAA wall stress analysis: 99-percentile versus peak stress. *Eur J Vasc Endovasc Surg* 2008;**36**(6):668–76.

41 Raut SS, Liu P, Finol EA. An Approach for Patient-Specific Multi-domain Vascular Mesh Generation Featuring Spatially Varying Wall Thickness Modeling. *J Biomech*

2015;**48**(10):1972–81.

42 Shang EK, Nathan DP, Woo EY, et al. Local wall thickness in finite element models improves prediction of abdominal aortic aneurysm growth. *J Vasc Surg* 2015;**61**(1):217–23.

43 Conlisk N, Geers AJ, McBride OMB, et al. Patient-specific modelling of abdominal aortic aneurysms: The influence of wall thickness on predicted clinical outcomes. *Med Eng Phys* 2016;**38**(6):526–37.

44 Biehler J, Wall WA. The impact of personalized probabilistic wall thickness models on peak wall stress in abdominal aortic aneurysms. *Int J Numer Methods Biomed Eng* 2018;**34**(2).

433 **Figure 1**. Steps of Finite Element Analyses

434 **Figure 2**. Flow Chart

435 **Figure 3**. Stress maps (first principal component) obtained with the FEA of the wall model

436 Patient 1

437 A1: pre-rupture, anterior view (min +0.062 [MPa]; max +0.752 [MPa])

438 B1: pre-rupture, posterior view (min +0.062 [MPa]; max +0.752 [MPa])

439 C1: rupture, anterior view (min +0.068 [MPa]; max +0.819 [MPa])

440 D1: rupture, posterior view (min +0.068 [MPa]; max +0.819 [MPa])

441

442 Patient 2

443 A2: pre-rupture, anterior view (min +0.079[MPa]; max +0.959[MPa])

444 B2: pre-rupture, posterior view (min +0.079[MPa]; max +0.959[MPa])

445 C2: rupture, anterior view (min +0.117[MPa]; max +1.404[MPa])

446 D2: rupture, posterior view (min +0.117[MPa]; max +1.404[MPa])

447

448 Patient 3

449 A3: pre-rupture, anterior view (min +0.068[MPa]; max +0.817[MPa])

450 B3: pre-rupture wall model, posterior view (min +0.068[MPa]; max +0.817[MPa])

451 C3: rupture wall model, anterior view (min +0.135[MPa]; max +1.625[MPa])

452 D3: rupture wall model, posterior view (min +0.135[MPa]; max +1.625[MPa])

453

454 Patient 4

455 A4: pre-rupture, anterior view (min +0.107[MPa]; max +1.295[MPa])

456 B4: pre-rupture, posterior view (min +0.107[MPa]; max +1.295[MPa])

457 C4: rupture, anterior view (min +0.096[MPa]; max +1.160[MPa])

458 D4: rupture, posterior view (min +0.096[MPa]; max +1.160[MPa])

459

460 Patient 5

461 A5: pre-rupture, anterior view (min +0.046[MPa]; max +0.554[MPa])

462 B5: pre-rupture, posterior view (min +0.046[MPa]; max +0.554[MPa])

463 C5: rupture, anterior view (min +0.052[MPa]; max +0.633[MPa])

464 D5: rupture, posterior view (min +0.052[MPa]; max +0.633[MPa])

465

466 **Figure 4.** Stress maps (first principal component, inner side of the wall) obtained with the FEA

467 of the thrombus model

468 Patient 1

469 A1: pre-rupture, anterior view (min +0.062 [MPa]; max +0.752 [MPa])

470 B1: pre-rupture, posterior view (min +0.062 [MPa]; max +0.752 [MPa])

471 C1: rupture, anterior view (min +0.068 [MPa]; max +0.819 [MPa])

472 D1: rupture, posterior view (min +0.068 [MPa]; max +0.819 [MPa])

473

474 Patient 2

475 A2: pre-rupture, anterior view (min -0.070 [MPa]; max +0.370 [MPa])

476 B2: pre-rupture, posterior view (min -0.070 [MPa]; max +0.370 [MPa])

477 C2: rupture, anterior view (min -0.172 [MPa]; max +0.379 [MPa])

478 D2: rupture, posterior view (min -0.172 [MPa]; max +0.379 [MPa])

479

480 Patient 3

481 A3: pre-rupture, anterior view (min -0.145 [MPa]; max +0.290 [MPa])

482 B3: pre-rupture, posterior view (min -0.145 [MPa]; max +0.290 [MPa])

C3: rupture, anterior view (min -0.143 [MPa]; max +0.572 [MPa])

D3: rupture, posterior view (min -0.143 [MPa]; max +0.572 [MPa])

Patient 4

A4: pre-rupture, anterior view (min -0.044 [MPa]; max +0.365 [MPa])

B4: pre-rupture, posterior view (min -0.044 [MPa]; max +0.365 [MPa])

C4: rupture, anterior view (min -0.111 [MPa]; max +0.389 [MPa])

D4: rupture, posterior view (min -0.111 [MPa]; max +0.389 [MPa])

Patient 5

A5: pre-rupture, anterior view (min -0.171 [MPa]; max +0.302 [MPa])

B5: pre-rupture, posterior view (min -0.171 [MPa]; max +0.302 [MPa])

C5: rupture, anterior view (min -0.031 [MPa]; max +0.343 [MPa])

D5: rupture, posterior view (min -0.031 [MPa]; max +0.343 [MPa])

Figure 5. CT scan and stress maps (first principal component) obtained with the FEA of ruptured AAA. The rupture site is visualized by the red circle;

Patient 1: A1, rupture anterior view of the thrombus model, (min +0.068 [MPa]; max +0.819 [MPa]); A2, rupture anterior view of the wall model (min +0.068 [MPa]; max +0.819 [MPa])

Patient 2: B1, rupture anterior view of thrombus model, (min -0.172 [MPa]; max +0.379 [MPa]); B2, rupture anterior view of the wall model (min +0.117[MPa]; max +1.404[MPa])

Patient 3: C1, rupture anterior view of the thrombus model, (min -0.143 [MPa]; max +0.572 [MPa]); C2, rupture anterior view of the wall model (min +0.135[MPa]; max +1.625[MPa])

507

508 Patient 5: D1, rupture anterior view of the thrombus model, (min -0.031 [MPa]; max +0.343
509 [MPa]); D2, rupture anterior view of the wall model (min +0.052[MPa]; max +0.633[MPa])

510

511

512

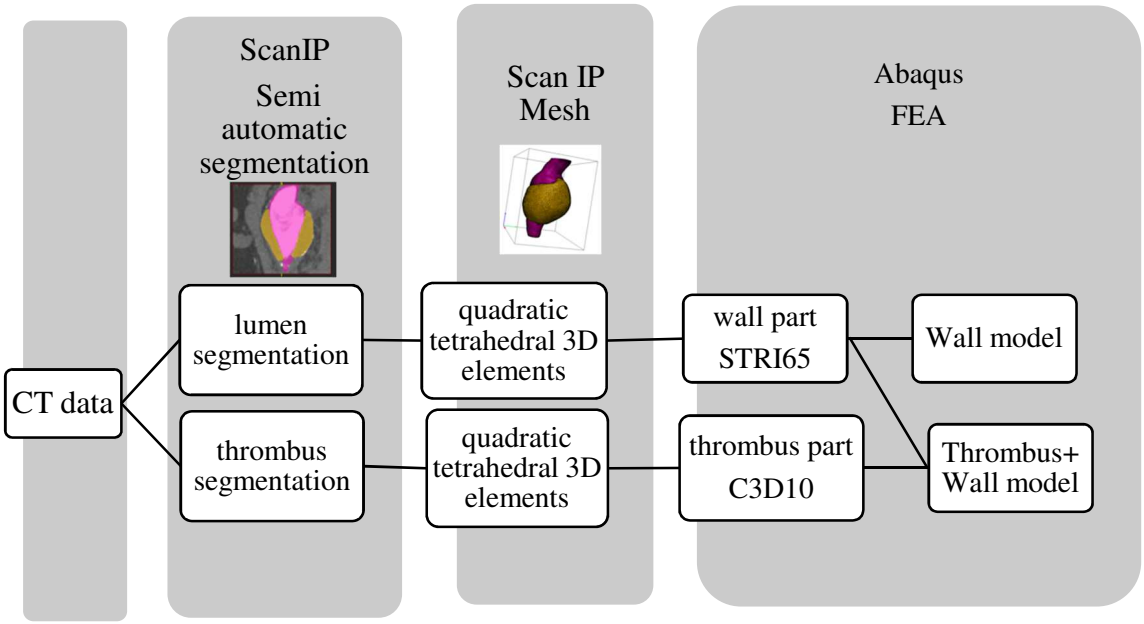
ScanIP
Semi
automatic
segmentation
Scan IP
Mesh
Abaqus
FEA
CT data
lumen
segmentation
thrombus
segmentation
quadratic
tetrahedral 3D
elements
quadratic
tetrahedral 3D
elements
wall part
STRI65
thrombus part
C3D10
Wall model
Thrombus+
Wall model

Figure 1.

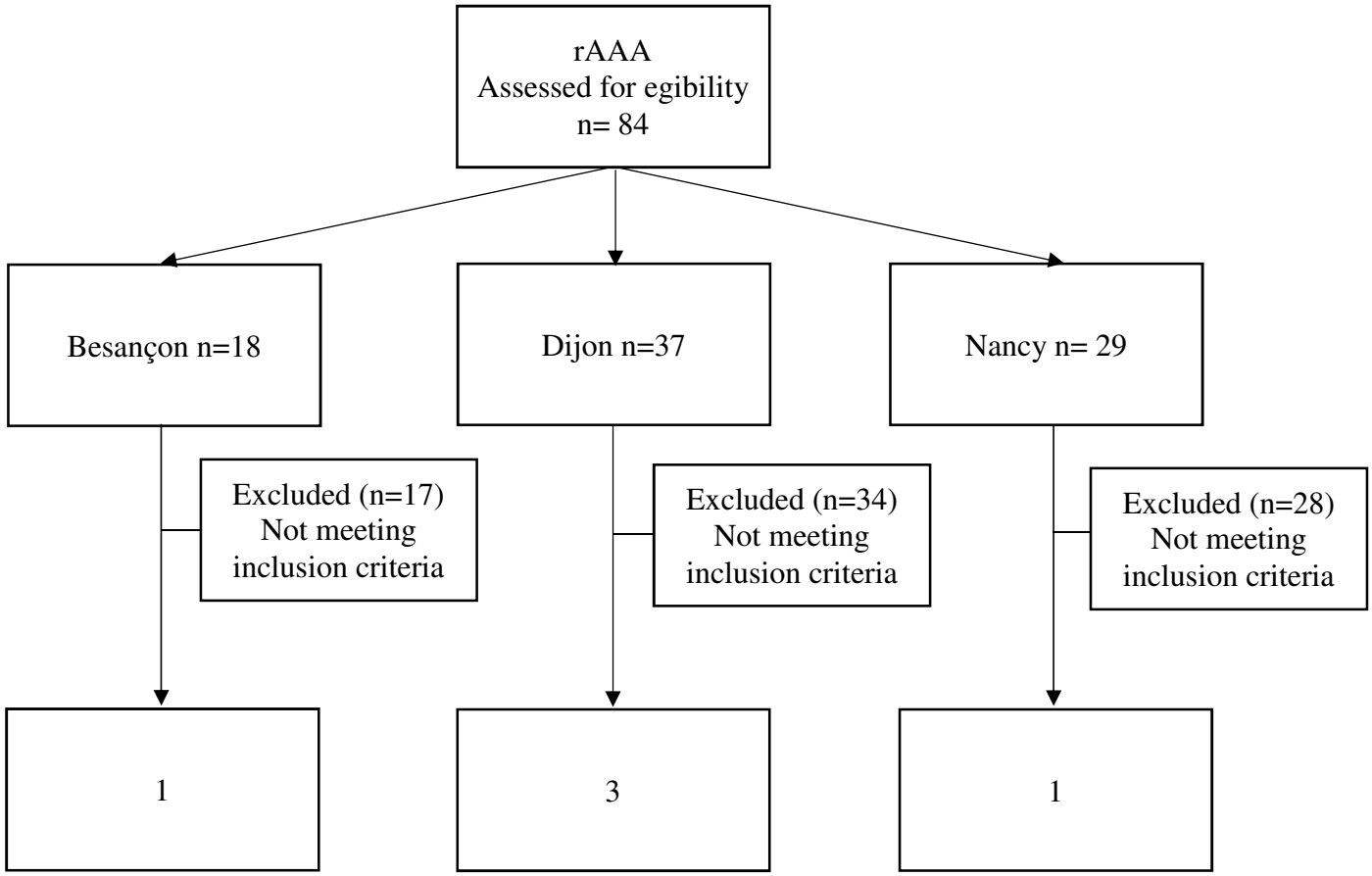
rAAA
Assessed for egibility
n= 84
Besançon n=18
Dijon n=37
Nancy n= 29
Excluded (n=17)
Not meeting
inclusion criteria
Excluded (n=34)
Not meeting
inclusion criteria
Excluded (n=28)
Not meeting
inclusion criteria
1
3
1

Figure 2.

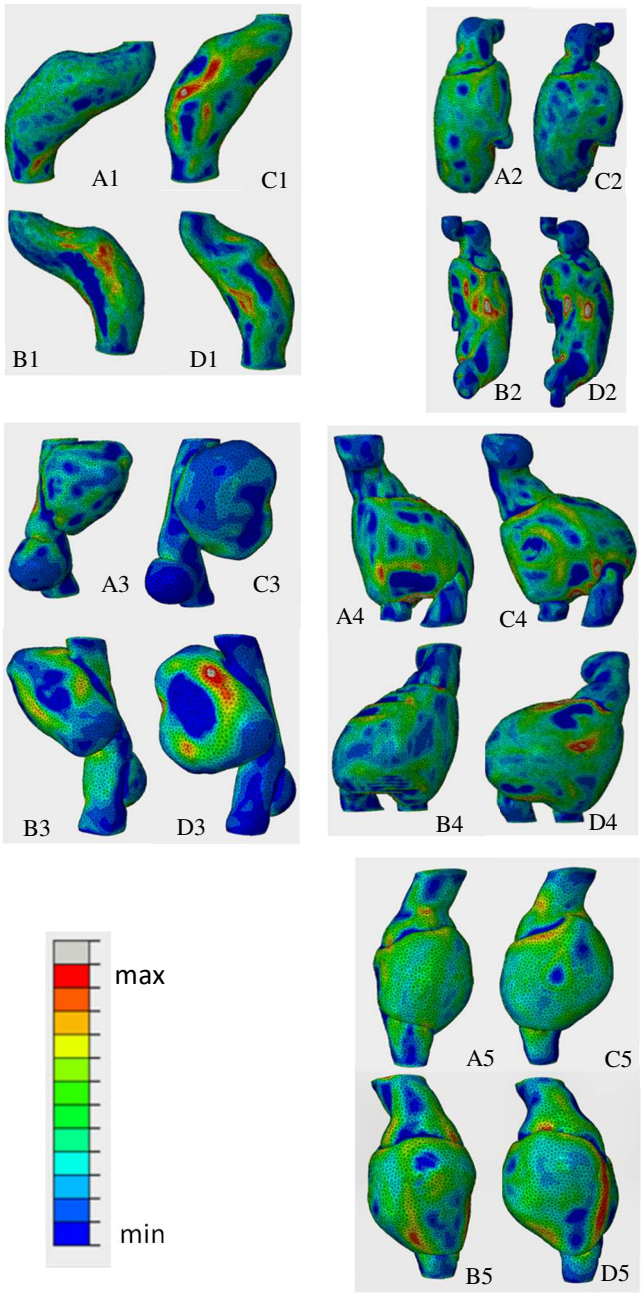

Figure 3.

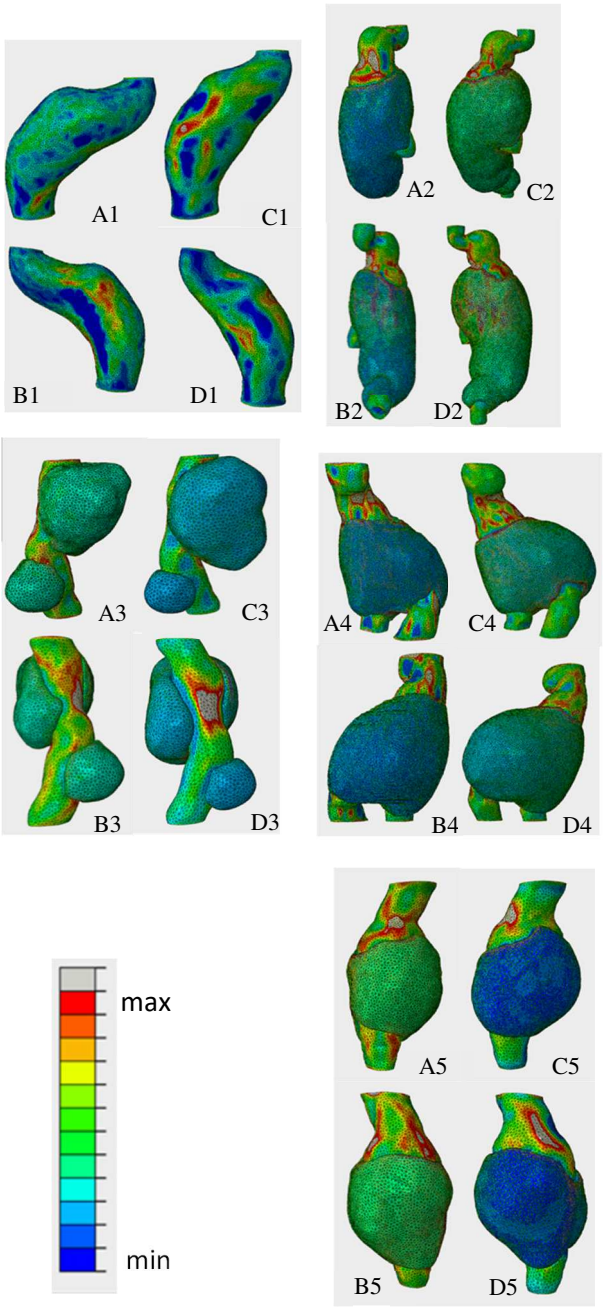

Figure 4.

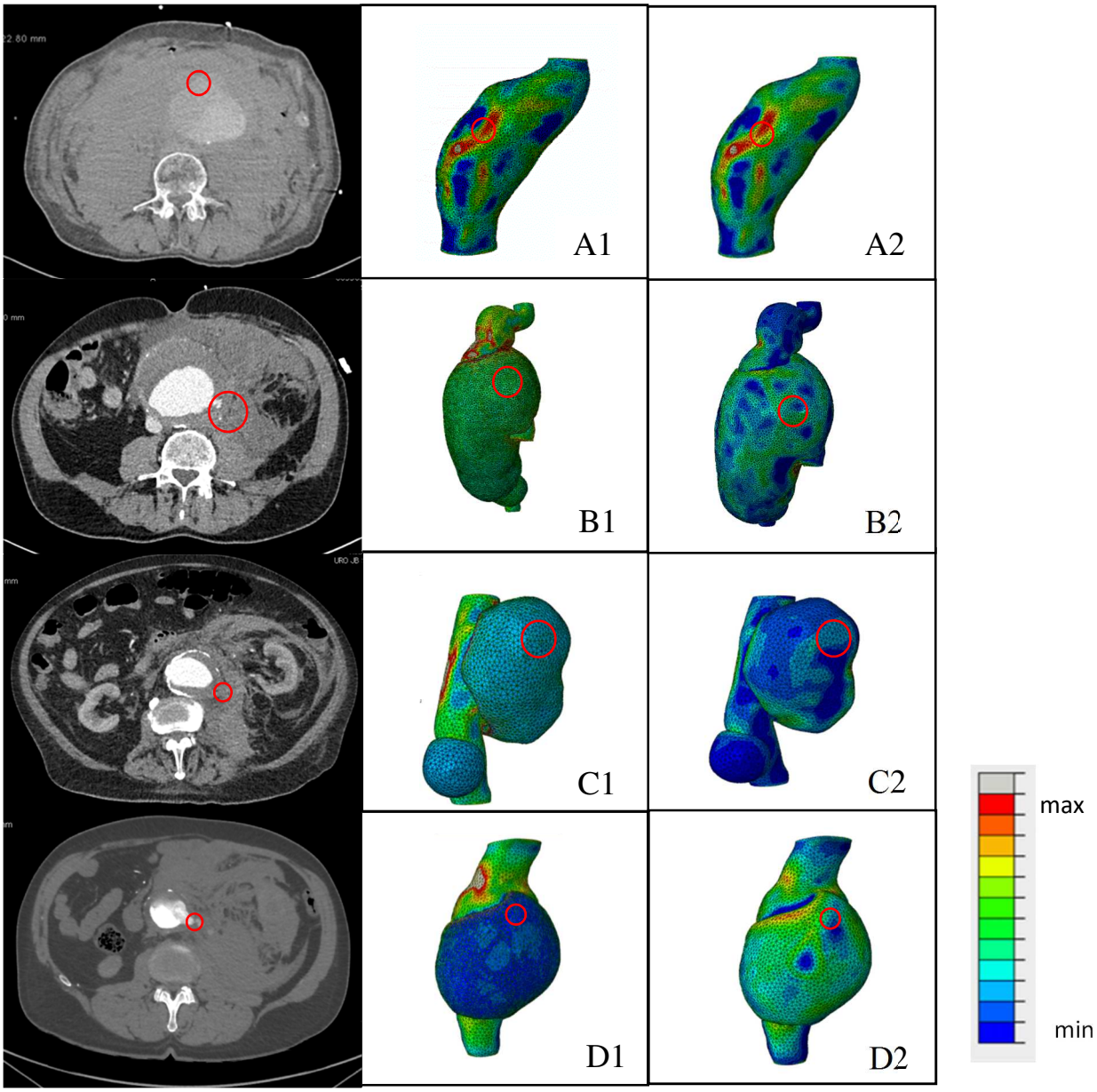

Figure 5.

Table I. Morphological data and FEA calculated parameters of AAA

Patient	CT scan data					Thrombus model		Wall model	
	MAD (mm)					99th percentile stress (MPa)			
	Time between the two CT scan (days)	AAA pre ruptured	AAA ruptured	CTA rupture location	PWS location	AAA pre ruptured	AAA ruptured	AAA pre ruptured	AAA ruptured
1	97	54	59	Right anterior	Right anterior	0.753	0.819	0.753	0.819
2	44	74	76	Left lateral	Third proximal	0.370	0.379	0.959	1.404
3	22	51	57	Left postero-lateral	Right lateral	0.291	0.572	0.817	1.625
4	36	90	97	-	Third proximal	0.365	0.390	1.295	1.160
5	90	53	58	Left postero lateral	Right and left antero lateral	0.303	0.343	0.555	0.633